# Reduction of the High Harmonics at the Electromagnetic Force and the Electromagnetic Torque in Synchronous Machines with Permanent Magnet

Tsvetomir Stoyanov
*General Electrical Engineering*
*Technical University of Sofia*
Sofia, Bulgaria
cmetodiev@tu-sofia.bg

Radoslav Spasov
*Electrical Machines*
*Technical University of Sofia*
Sofia, Bulgaria
rls@tu-sofia.bg

Plamen Rizov
*Electrical Machines*
*Technical University of Sofia*
Sofia, Bulgaria
pmri@tu-sofia.bg

***Abstract*— This paper presents the results from a study of permanent magnet synchronous machines, with magnets positioning in the rotor form like "V". The following types of stator winding (these are the main possibilities for these values of stator slots -Z and pair of poles-p) are investigated: Case 1- three-phase, single-layer, full-pitch coil, integral-slot stator winding (3FFPW); Case 2- three-phase, double-layer, short-pitch coil, integral-slot stator winding (3FSPW); Case 3- three-phase, single-layer, full-pitch coil, skew slots, integral-slot stator winding (3FSSW); Case 4- five-phase, double-layer, short-pitch coil, fractional-slot stator winding (5FSPW). The conducted analysis is based on the application of finite element method. The benchmark for the results obtained are the amplitude of the first harmonic of the e.m.f. and electromagnetic torque and harmonic order. The research in this article is based on the application of the 2D software computer package FEMM 4.2.**

***Keywords—permanent magnet with "V" form, synchronous machine, finite element method, stator's winding.***

## I. INTRODUCTION

On the one hand, there are many and various requirements for electrical machines used as drives for hybrid cars – high level of efficiency, capacity to overload up to twice, minimum ripple of the electromagnetic torque. On the other hand it is imperative that the inspection to meet these requirements be increased at the design stage. Many methods can be used for this purpose - analytical, numerical, simulation and experimental. The electric drive of the hybrid vehicle can be realized with different types of electric motors. The selection of electric motor (synchronous, asynchronous or brushless DC electric motor) will depend on the choice of the constructor, after assessing the advantages and disadvantages of each type of electric motor. The common among all electric drives, regardless of the type of electric motor, is that they'll operate at high electrical, magnetic and thermal loads, which requires to create highly efficient electric drive, but this also raises a number of problems to solve. The most complete requirements for electric machines for propulsion of hybrid vehicles are satisfied by synchronous machines with permanent magnets in the rotor (SMPM- Fig.1), because they have many of the necessary advantages [1, 2]. These benefits can be achieved using different approaches: different methods of time control of the amplitude, shape of current and voltage or sensorless field oriented control [3], a multiplicity of types of the stator winding [4], or a different rotor and stator geometries. This paper presents the results from study of SMPM with a different type of stator winding but with absolutely the same stator and rotor geometry that eliminates the influence of the tooth slot ratio.

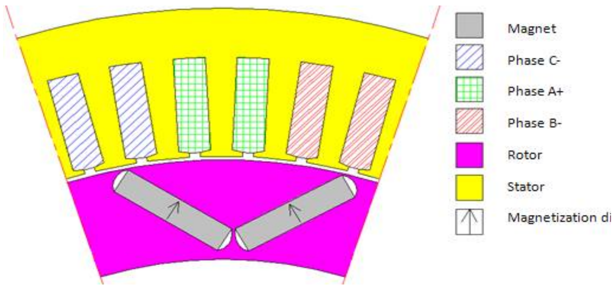


The paper presents the configuration of the machine and the calculations to determine the winding factor. The distribution of the electromagnetic field in the machine is determined by the finite element method, and the results are used to calculate the electromagnetic torque and electromagnetic force.

## II. MACHINE CONFIGURATION

The machine configuration is shown on Fig.2. The numerical data about the machine's dimensions and parameter corresponding to the different stator winding types are presented in Table 1.

The skewing of the slots is simulated in the following

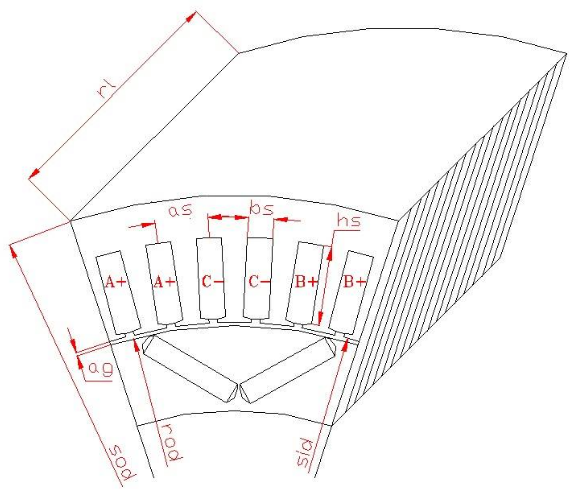


Fig. 2. The machine configuration

978-1-7281-2697-5/19/$31.00 ©2019 IEEE

way: the first considered case is when the winding is 3FFPW (Fig.3a-case 1). The rotor is then rotated to three geometric degrees clockwise relative to case 1 (Fig.3b - Case 2). The last rotation of the rotor is three geometric degrees counter clockwise versus case 1 (Figure 3c - Case 3). These three degrees are half the distance between the two stator slots, which is six degrees.

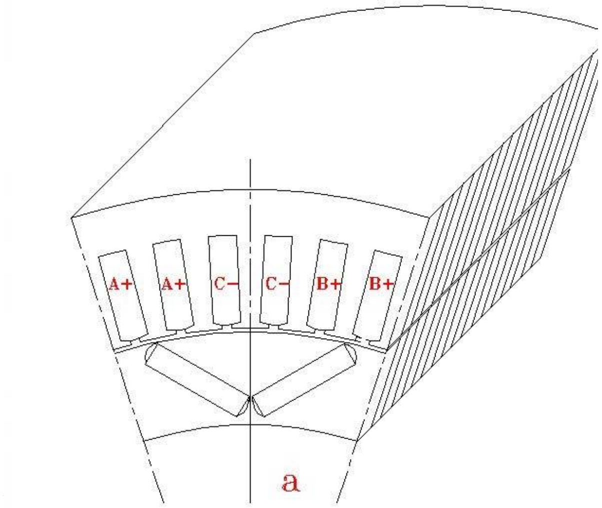


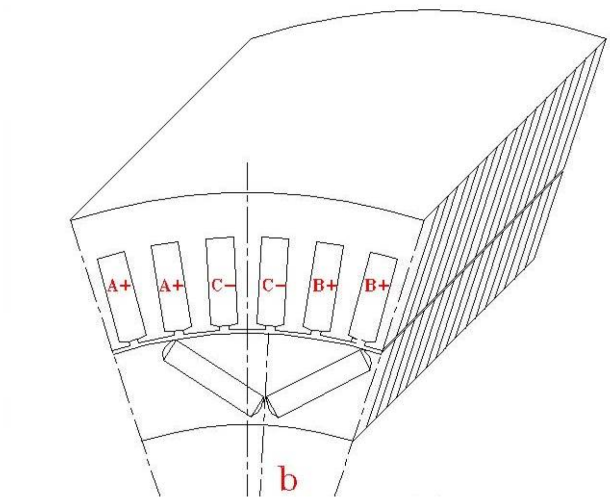


Fig. 3b. Simulation of the slot's skewing.

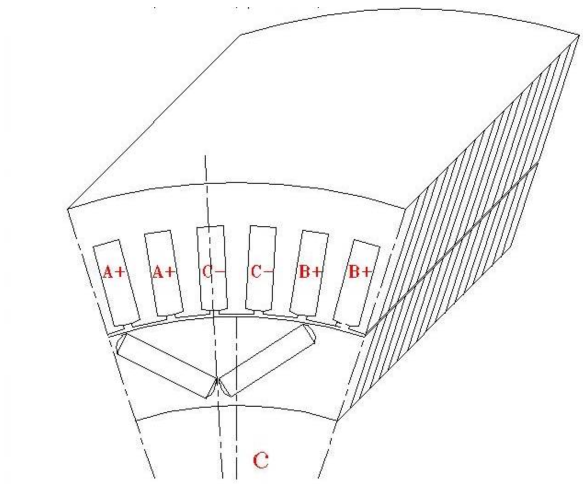


Fig. 3c. Simulation of the slot's skewing.

TABLE I. THE NUMERICAL DATA ABOUT THE MACHINE'S DIMENSIONS AND PARAMETER

| Case | | 1-3FFPW | 2-3FSPW | 3-3FSSW | 4-5FSPW |
|---|---|---|---|---|---|
| q | | 2 | 2 | 2 | 6/5 |
| Phase | | 3 | 3 | 3 | 5 |
| Coil path | | 6-full | 5-short | 6-full | - |
| Layer | | single | double | single | single |
| Z | | 60.0 | | | |
| ag | mm | 0.70 | | | |
| rl | mm | 90.0 | | | |
| as | deg | 30.0 | | | |
| bs | mm | 5.80 | | | |
| hs | mm | 18.10 | | | |
| sod | mm | 242.0 | | | |
| sid | mm | 184.20 | | | |
| rod | mm | 182.80 | | | |

The calculation of electromagnetic torque is through expression (1). The calculations are similar for e.m.f.

$$M = \frac{M_{C1}}{3} + \frac{M_{C2}}{3} + \frac{M_{C2}}{3} \text{ [N.m]}, \quad (1)$$

where $M_{C1}$ is the electromagnetic torque in case 1, $M_{C2}$ is the electromagnetic torque in case 2 and $M_{C3}$ is the electromagnetic torque in case 3.

The diagrams of the windings which covers two poles and three phases are shown from Fig.4 to Fig.5 (Fig.4-3FFPW and 3FSSW; Fig5-3FSPW). Fig.6 -5FSPW presents part of the coil's connections of the phase "A" and phase "B". The use of this winding is not recommended because the coils are of different coil-span and the phase's e.m.f. are not symmetrical. On Fig.7 to Fig.9, where with Z are marked the slots number, T marks the top layer of the slot and B marks the bottom layer of the slot, are presented the full diagrams of the machines winding's (Fig.7-3FFPW and 3FSSW; Fig.8-3FSPW; Fig.9-5FSPW).

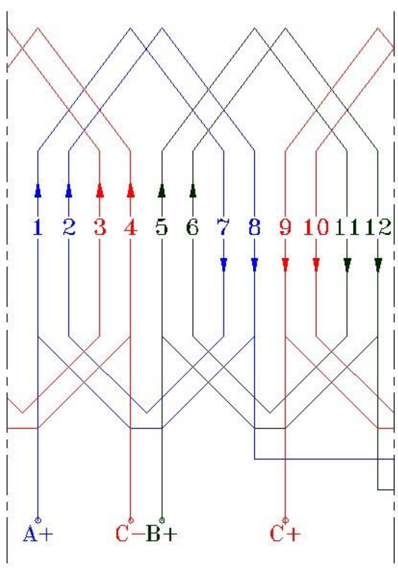


Fig. 4. Diagram of the winding for 3FFPW and 3FSSW

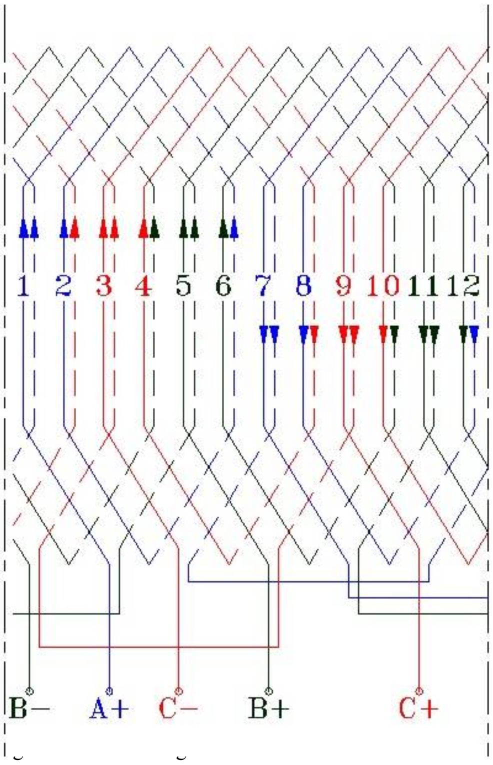


Fig. 5.

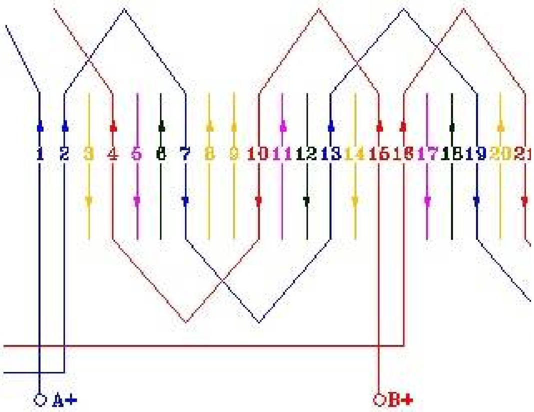


Fig. 6. Diagram of the winding for 5FSPW

| Z | 1 | 2 | 3 | 4 | 5 | 6 | 7 | 8 | 9 | 10 |
|---|---|---|---|---|---|---|---|---|---|---|
| | A+ | A+ | B- | B- | C+ | C+ | A- | A- | B+ | B+ |
| Z | 11 | 12 | 13 | 14 | 15 | 16 | 17 | 18 | 19 | 20 |
| | C- | C- | A+ | A+ | B- | B- | C+ | C+ | A- | A- |
| Z | 21 | 22 | 23 | 24 | 25 | 26 | 27 | 28 | 29 | 30 |
| | B+ | B+ | C- | C- | A+ | A+ | B- | B- | C+ | C+ |
| Z | 31 | 32 | 33 | 34 | 35 | 36 | 37 | 38 | 39 | 40 |
| | A- | A- | B+ | B+ | C- | C- | A+ | A+ | B- | B- |
| Z | 41 | 42 | 43 | 44 | 45 | 46 | 47 | 48 | 49 | 50 |
| | C+ | C+ | A- | A- | B+ | B+ | C- | C- | A+ | A+ |
| Z | 51 | 52 | 53 | 54 | 55 | 56 | 57 | 58 | 59 | 60 |
| | B- | B- | C+ | C+ | A- | A- | B+ | B+ | C- | C- |
| | N | | | | | S | | | | |

Fig. 7. The diagram of the 3FFPW and 3FSSW

| Z | 1 | 2 | 3 | 4 | 5 | 6 | 7 | 8 | 9 | 10 |
|---|---|---|---|---|---|---|---|---|---|---|
| T | A+ | B- | B- | C+ | C+ | A- | A- | B+ | B+ | C- |
| B | A+ | A+ | B- | B- | C+ | C+ | A- | A- | B+ | B+ |
| Z | 11 | 12 | 13 | 14 | 15 | 16 | 17 | 18 | 19 | 20 |
| T | C- | A+ | A+ | B- | B- | C+ | C+ | A- | A- | B+ |
| B | C- | C- | A+ | A+ | B- | B- | C+ | C+ | A- | A- |
| Z | 21 | 22 | 23 | 24 | 25 | 26 | 27 | 28 | 29 | 30 |
| T | B+ | C- | C- | A+ | A+ | B- | B- | C+ | C+ | A- |
| B | B+ | B+ | C- | C- | A+ | A+ | B- | B- | C+ | C+ |
| Z | 31 | 32 | 33 | 34 | 35 | 36 | 37 | 38 | 39 | 40 |
| T | A- | B+ | B+ | C- | C- | A+ | A+ | B- | B- | C+ |
| B | A- | A- | B+ | B+ | C- | C- | A+ | A+ | B- | B- |
| Z | 41 | 42 | 43 | 44 | 45 | 46 | 47 | 48 | 49 | 50 |
| T | C+ | A- | A- | B+ | B+ | C- | C- | A+ | A+ | B- |
| B | C+ | C+ | A- | A- | B+ | B+ | C- | C- | A+ | A+ |
| Z | 51 | 52 | 53 | 54 | 55 | 56 | 57 | 58 | 59 | 60 |
| T | B- | C+ | C+ | A- | A- | B+ | B+ | C- | C- | A+ |
| B | B- | B- | C+ | C+ | A- | A- | B+ | B+ | C- | C- |
| | N | | | | | S | | | | |

Fig. 8. The diagram of the 3FSPW

| Z | 1 | 2 | 3 | 4 | 5 | 6 | 7 | 8 | 9 | 10 |
|---|---|---|---|---|---|---|---|---|---|---|
| | A+ | A+ | D- | B+ | E- | C+ | A- | D+ | D+ | B- |
| Z | 11 | 12 | 13 | 14 | 15 | 16 | 17 | 18 | 19 | 20 |
| | E+ | C- | A+ | D- | B+ | B+ | E- | C+ | C+ | A- |
| Z | 21 | 22 | 23 | 24 | 25 | 26 | 27 | 28 | 29 | 30 |
| | D+ | B- | E+ | E+ | C- | A+ | D- | B+ | E- | C+ |
| Z | 31 | 32 | 33 | 34 | 35 | 36 | 37 | 38 | 39 | 40 |
| | C+ | A- | A- | D+ | B- | E+ | C- | A+ | D- | D- |
| Z | 41 | 42 | 43 | 44 | 45 | 46 | 47 | 48 | 49 | 50 |
| | B+ | E- | C+ | A- | D+ | B- | B- | E+ | C- | C- |
| Z | 51 | 52 | 53 | 54 | 55 | 56 | 57 | 58 | 59 | 60 |
| | A+ | D- | B+ | E- | E- | C+ | A- | D+ | B- | E+ |
| | N | | | | | S | | | | |

Fig. 9. The diagram of the 5FSPW

## III. DETERMINING OF THE WINDING FACTOR

A number of authors present a methodology for determining of winding factor [5, 6, 7], which is used in the calculation of the e.m.f. Here it is presented in a summarized form (by the expressions from (2) to (6)) and then applied with data about the investigated windings - Table 2.

### *A. Pitch Factor*

**The pitch factor is noted with $k_p$** and represents the ratio of vector (phasor) sum of the induced electromotive force (e.m.f.) per coil to the arithmetical sum of induced e.m.f. If the coil span is equal to pole pitch, then $k_p=1$, otherwise $k_p$ is less than one. The following assumptions are made:

- If the coil is full pitched, in this case the resultant e.m.f is equal to ***2E***.
- If the coil is chorded (at an angle $\theta$ in electrical degree), in this case the resultant e.m.f is equal to $E_R$ (sum of two voltages).

$$E_R = 2E\cos\frac{\theta}{2} \tag{2}$$

Then the pitch factor is equal to:

$$k_p = \frac{2E\cos\frac{\theta}{2}}{2E} = \cos\frac{\theta}{2} \tag{3}$$

*B. Distribution Factor*

**The distribution factor is noted with $K_d$** and represents the ratio of vector (phasor) sum of the induced electromotive force (e.m.f.) in the all coils covered by one pole to the arithmetical sum of induced e.m.f in all coils concentrated in one slot under one pole (if the winding has concentrated construction). If the number of slots per pole per phase is equal to one, then $k_d=1$, otherwise $k_d$ is less than one. . The following assumptions are made:

- If the slots covered by one pole are marked with $Q$ and slots per pole and phase with $q$, in this case the induced electromotive force (e.m.f.) of the each side of the coil is $2E$.
- It is assumed that the angle between two slots is:

$$\gamma = \frac{180^0}{Q} \tag{4}$$

Then the distribution factor is equal to:

$$k_d = \frac{\sin\frac{q\gamma}{2}}{q\sin\frac{\gamma}{2}} \tag{5}$$

*C. Winding factor*

The winding factor is equal to the product of pitch factor and distribution factor:

$$k_w = k_q k_d \tag{6}$$

## IV. Analysis

There is a huge variety of methods for analyzing rotating electric machines, each having its advantages and disadvantages. The method based on fragmentation of the studied area into smaller elements is one way to achieve initial results without creating a real machine. For this purpose, a number of software products have been developed- FEMM 4.2, Ansys Maxwell 2015, QuickField. In turn, they are used in research by a number of authors in conducting their research [8, 9]. Thanks to the product FEMM 4.2 in the article the magnetic field distribution is obtained and on its basis it is possible to determine the harmonic order of e.m.f and electromagnetic torque. The harmonic order and the amplitude of the first harmonic is the basis for comparison of the different types of stator's winding. Part of the modeled machine (one pair of poles) is represented by Fig.10. In the middle of the air gap is built an arc serving to determine the electromagnetic torque.

TABLE II. PITCH FACTOR, DISTRIBUTION FACTOR AND WINDING FACTOR

| Case | 1-3FFPW | 2-3FSPW | 3-3FSSW | 4-5FSPW |
|---|---|---|---|---|
| $k_p$ | 1.00000 | 0.96593 | 1.00000 | 0.96593 |
| $k_d$ | 0.96593 | 0.96593 | 0.96593 | 0.99496 |
| $k_w$ | 0.96593 | 0.93301 | 0.96593 | 0.96106 |

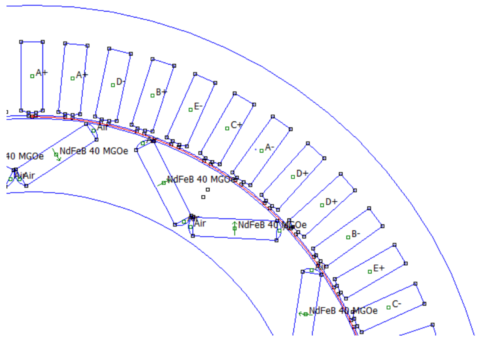

Fig. 10. Part of the modeled machine (one pair of poles)

A solution has been made for a time span of 20 milliseconds. The period is divided into forty steps. The interval between steps is the same. The study was conducted at a current density of 30 A/mm$^2$. The current density values for the initial time point are presented in Table 3.

The harmonic order (higher harmonics) of the electromotive force is presented on Fig.11. The same dependency for ripple of the electromagnetic torque is presented on Fig.12. The amplitude of the main harmonics - Table 4. The torque as time function is presented on Fig.13.

TABLE III. THE CURRENT DENSITY VALUES FOR THE INITIAL TIME POINT

| Case | 1-3FFPW | 2-3FSPW | 3-3FSSW | 4-5FSPW |
|---|---|---|---|---|
| $J_A$ | $J_{MAX}$ | $J_{MAX}$ | $J_{MAX}$ | $J_{MAX}$ |
| $J_B$ | $-0.5J_{MAX}$ | $-0.5J_{MAX}$ | $-0.5J_{MAX}$ | $0.31J_{MAX}$ |
| $J_C$ | $-0.5J_{MAX}$ | $-0.5J_{MAX}$ | $-0.5J_{MAX}$ | $-0.81J_{MAX}$ |
| $J_D$ | - | - | - | $-0.81J_{MAX}$ |
| $J_E$ | - | - | - | $0.31J_{MAX}$ |

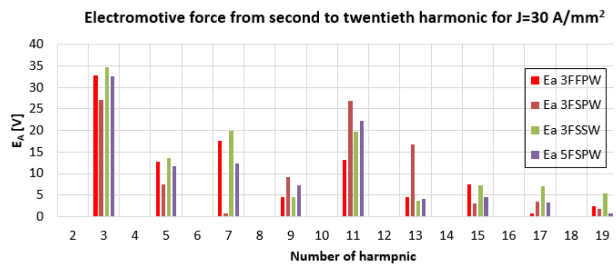

Fig. 11. The harmonic order of e.m.f

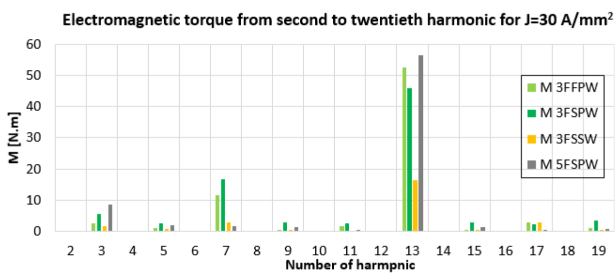

Fig. 12. The harmonic order of torque.

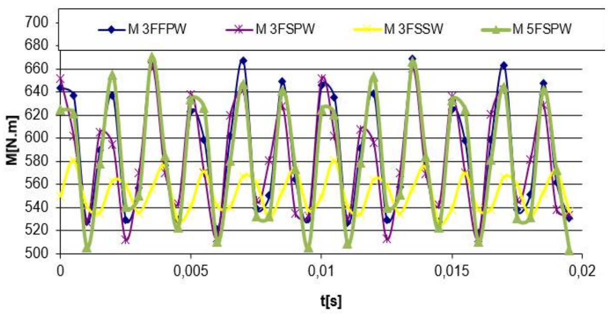

Fig. 13. The torque as time function.

TABLE IV. MAIN HARMONICS OF THE TORQUE AND E.M.F

| $E_A$ [V] | | | |
|---|---|---|---|
| 1-3FFPW | 2-3FSPW | 3-3FSSW | 4-5FSPW |
| 391.4321 | 350.7968 | 390.2992 | 380.7605 |
| M [N.m] | | | |
| 1-3FFPW | 2-3FSPW | 3-3FSSW | 4-5FSPW |
| 586.611 | 580.8212 | 551.1878 | 581.3434 |

## V. CONCLUSIONS

This paper presents the results from a study of stator winding and the following more important conclusions are drawn. From the results, shown on Fig. 11 to Fig. 13 and Table 4, it can be seen that the highest amplitude of the e.m.f. is obtained by the winding 3FFPW, followed by 3FSSW. The torque amplitude leader is again the configuration 3FFPW, followed by 5FSPW. The torque ripples at 3FFPW, 3FSPW and 5FSPW are completely identical, but their amplitude is significantly lower at 3FSSW (Fig. 12). The use of the 5FSPW is not recommended, because the coils are with different coil-span and the phase's e.m.f. are not symmetrical. The obtained conclusions are based on the comparison of the first harmonic amplitude, the amplitudes of higher harmonics in the harmonic order and the torque ripples.

## ACKNOWLEDGMENT


The authors would like to thank the Research and Development Sector at the Technical University of Sofia for the financial support.


## REFERENCES


[1] D. Zhu, Wang, S. Lee, Y. Cho, Hall effect sensor based space vector PWM control of permanent magnet synchronous machine, International Journal of Applied Electromagnetics and Mechanics 39 (2012), pp. 919–924.

[2] J. Li, , S. Li, X. Chen, Adaptive speed control of a PMSM servo system using an RBFN disturbance observer, Transactions of the Institute of measurement and control, 2011.

[3] E. Rachev, V. Petrov, An approach to solving ramp start issues in sensorless field oriented control with sliding mode observer for permanent magnet synchronous motors, Proceedings of XVI International conference on electrical machines, drives and power system (ELMA 2019), pp. 238 – 241, ISBN: 978-1-7281-1412-5.

[4] Soleimani, J. , A. Vahedi, IPM Synchronous motor for traction applications: performance analysis considering airgap variation, PRZEGLĄD ELEKTROTECHNICZNY, ISSN 0033-2097, 2012.

[5] R. Krall, J. Krenn and H. Weiss, Six phase permanent magnet machine with fractional slot concentrated winding, https://pure.unileoben.ac.at/portal/files/1071185/Six_Phase_Permanent_Magnet_Machine_with_Fractional_Slot_Concentrated_Winding.pdf.

[6] A. Tommaso, F. Genduso, R. Miceli, A software for the evaluation of winding factor harmonic distribution in high efficiency electrical motors and generators, https://www.researchgate.net/publication/261320497_A_software_for_the_evaluation_of_winding_factor_harmonic_distribution_in_high_efficiency_electrical_motors_and_generators, 2003.

[7] S. Shahl, Electrical machines II, https://www.slideshare.net/aswardi/i-introduction-39125212.

[8] G. Todorov, Loss distribution in IPMSM at different control strategy, X-th Electrical Engineering Faculty Conference, 2018, DOI: 10.1109/BULEF.2018.8646958.

[9] V. Lazarov, Z. Zarkov. I. Bachev, Determination of the synchronous inductances of a claw pole alternator, Proceedings of XVI International conference on electrical machines, drives and power system (ELMA 2019), pp. 535 – 540, ISBN: 978-1-7281-1412-5.